Pergamon

Tetrahedron Letters 41 (2000) 7917–7920

TETRAHEDRON LETTERS

Mapping of the highest occupied molecular orbital of a DNA–RNA hybrid by cobalt–benzoyl peroxide oxidation

Takashi Nakamura and Isao Saito*

Department of Synthetic Chemistry and Biological Chemistry, Faculty of Engineering, Kyoto University, Kyoto 606-8501, Japan and CREST, Japan Science and Technology Corporation

Received 28 June 2000; revised 21 July 2000; accepted 10 August 2000

Abstract

Ab initio calculations of the highest occupied molecular orbital (HOMO) of the guanine (G)-containing sequences with DNA–RNA hybrid geometry were performed at the HF 6-31G* level. Sequence dependent guanine oxidation with Co(II) and benzoyl peroxide (BPO) has been observed for a DNA–RNA hybrid as revealed by PAGE analysis of the reaction mixture after hot piperidine treatment. The DNA cleavage of 5′-GGG-3′ sequence was consistent with the selectivity predicted from calculated HOMOs of 5′-GGG-3′ sequence.

The highest occupied molecular orbital (HOMO) of organic molecules plays an important role in chemical reactions by interacting with the lowest unoccupied molecular orbital (LUMO) of reactant molecules.[1] Previously, we reported the first experimental HOMO mapping of a B-DNA duplex using Co(II) and benzoyl peroxide (BPO), in combination with ab initio calculations of various guanine (G)-containing DNA sequences.[2] We therein suggested an important but unestablished binding force, the interaction of the HOMO of duplex DNA with the LUMO of DNA binding molecules such as metal ions, drugs and proteins. The DNA–RNA hybrid plays a key roles in transcription,[3] DNA replication,[4] and in the synthesis of retroviral cDNA by reverse transcription.[5] The HOMO location of the DNA–RNA hybrid might be very useful for understanding the recognition mechanism by drugs and proteins. We herein report the result of experimental HOMO mapping of DNA–RNA hybrid using Co(II) and BPO that was consistent with the calculated results.

Ab initio calculations of HOMOs of DNA–RNA hybrid and B-DNA duplex were performed at the HF/6-31G* level using GAUSSIAN94[6] as mentioned previously.[2,7] The orbital contour plots of the calculated HOMOs of typical 5-mers of the B-DNA duplex and the DNA–RNA hybrid are shown in Fig. 1. As seen in Fig. 1d, the HOMO of DNA–RNA hybrid 5′-

* Corresponding author.

0040-4039/00/$ - see front matter
PII: S0040-4039(00)01380-0

d(TGGGT)-3′/5′-r(ACCCA)-3′ is localized on the 5′-G with almost no HOMO on the other Gs. The HOMO of 5′-GG-3′ sequence was also localized exclusively on the 5′-G of 5′-GG-3′ sequence (Fig. 1b). These results were different from those of B-form DNA (Fig. 1a,c). It is proposed that the overall structure of the DNA–RNA hybrid is close to A-form, although the minor groove of hybrid duplexes is narrower than that of RNA duplex.[8,9] The A-form duplex is more compact than the B-form duplex because the bases are tilted with regard to the helical axis and therefore there are more base pairs per turn. The minor groove of the A-form duplex, a major point of contact for proteins, is wider and shallower than the B-form duplex. In contrast, the major groove is less accessible, because it is much deeper and phosphate groups overhang it. Therefore, the individual bases are buried deep in the groove. As a result, the enormous change of stacking between guanine and guanine might induce the drastic change of the HOMO location.

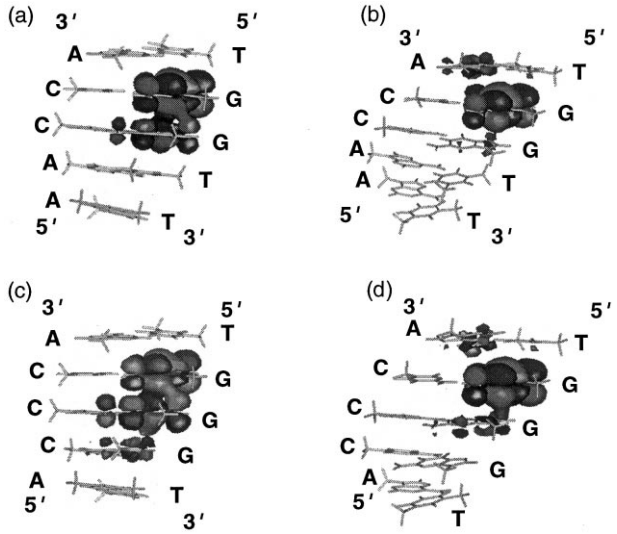

Figure 1. Orbital contour plots of the HOMOs of two B-form DNA 5-mers (a, c) and the corresponding DNA–RNA hybrid 5-mers (b, d) obtained by ab initio calculation using GAUSSIAN94[6] at the HF/6-31G* level. The sequences are shown on both sides. The sugar backbones were replaced by methyl group[7]

In order to confirm whether the DNA–RNA hybrid adopts an A-form-like conformation under DNA cleavage conditions, the circular dichroism (CD) spectrum of a DNA–RNA hybrid 33 mer 5′-d(CGTTATCATTGGTTATCATTGGGTTATCATTCG)-3′/5′-r(CGAAUGAUA-ACCCAAUGAUAACCAAUGAUAACG)-3′ was measured (Fig. 2). As shown in Fig. 2, the conformational change between the DNA duplex and the DNA–RNA hybrid was clearly observed. It was thus confirmed that the DNA–RNA hybrid is completely changed to an A-form-like conformation. From high resolution DNA crystal structural analysis, it was reported that $Co(NH_3)_6^{3+}$ binds to the O_6/N_7 sites of guanine bases at the major groove side of GpG step via hydrogen bonds in A-DNA.[10,11] Therefore, it is likely that Co(II) is accessible to the guanines in the major groove of the DNA–RNA hybrid and that Co(II) and BPO oxidation (experimental HOMO mapping) is available for the DNA–RNA hybrid.

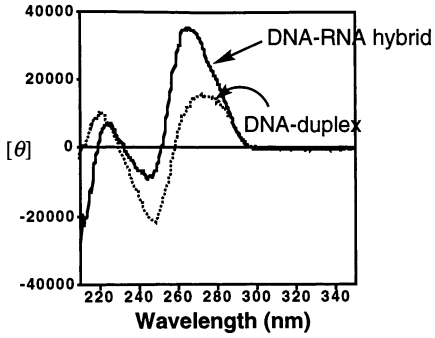

Figure 2. CD spectra of DNA–RNA hybrid (solid line) and the corresponding DNA duplex (dotted line) (100 μM base concentration) in 10 mM sodium cacodylate buffer (pH 7.0) and 100 mM NaCl at 37°C. Hybridization was achieved by heating the samples to 90°C for 5 min and then slowly cooling to room temperature. CD data were transformed into molar ellipticity [θ] in the units of degree cm^2/dm of monomer subunits

The DNA cleavage experiment was examined next. Incubation of the double-stranded ^{32}P-5′-end-labeled DNA duplex or DNA–RNA hybrid with Co(II) ion ($CoCl_2$, 10 μM) and BPO (50 μM) at 37°C for 5 min, followed by treatment with hot piperidine, resulted in a highly selective G cleavage (Fig. 3). The extent of strand cleavage was determined using a densitometric

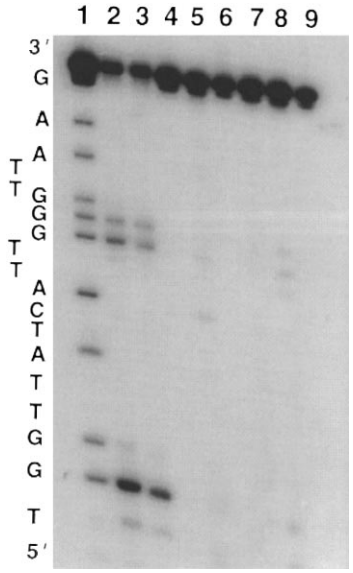

Figure 3. Autoradiograph of a denaturing gel electrophoresis for ^{32}P-5′-end-labeled ODN 5′-CGTTATCATTGGT-TATCATTGGGTTATCATTCG-3′ sequence after incubation of the duplex in the presence of Co(II) and benzoyl peroxide (BPO). ^{32}P-5′-end-labeled ODN 33-mer was hybridized to the complementary strand (DNA or RNA, 2.5 μM, strand concentration) in 10 mM sodium cacodylate buffer, pH 7.0. Hybridization was achieved by heating the sample at 90°C for 5 min and slowly cooling to room temperature. The ^{32}P-5′-end-labeled ODN duplex or DNA–RNA hybrid (2.0×10^{-5} cpm) containing Co(II) (10 μM) and BPO (50 μM) was incubated at 37°C for 5 min. After piperidine treatment (90°C, 20 min), the sample was dried and electrophoresed through a denaturing 12% polyacrylamide/7 M urea gel. (Lane 1) Maxam–Gilbert sequencing reactions G+A; (lanes 2, 3) incubated in the presence of $CoCl_2$ and BPO; (lanes 4, 7) incubated with $CoCl_2$; (lanes 5, 8) incubated with BPO; (lanes 6, 9) DNA, dark control, no piperidine treatment. Lanes 2, 4, 5 and 6 show the results of DNA–RNA hybrid, whereas lanes 3, 7, 8 and 9 are for the corresponding DNA duplex

assay. For direct comparison with the calculated HOMO data, the cleavage data were normalized by assigning a value of 100 to the largest cleavage band in 5′-TGGGT-3′. As seen in Fig. 3, the 5′-TGGGT-3′ cleavage was notable, since there was almost no difference in B-DNA and DNA–RNA hybrid in 5′-GG-3′ step cleavage (lane 2 vs 3). The DNA cleavage pattern for 5′-GGG-3′ of the DNA–RNA hybrid was more 5′-G selective than that for the DNA duplex (Table 1). The DNA cleavage pattern was consistent with the calculated HOMOs of the 5′-GGG-3′ sequences, although the experimental data did not completely match with the calculated HOMOs.[12]

Table 1
Relative intensities (G_1:G_2)[a] for 5′-$G_1G_2G_3$-3′ site cleavage

B-form duplex (lane 3)	DNA–RNA hybrid (lane 2)
100:71	100:**56**

[a] The intensities were normalized by assigning a value of 100 to the largest cleavage band (at G_1 site).

In conclusion, the present study has demonstrated that Co(II) and BPO oxidation is available for the HOMO mapping of the DNA–RNA hybrid as well as for the B-form DNA duplex. Therefore, this method would be useful for HOMO mapping of other DNA, RNA or DNA–RNA hybrid structures.

References

1. Fukui, K. *Acc. Chem. Res.* **1971**, *4*, 57–64.
2. Saito, I.; Nakamura, T.; Nakatani, K. *J. Am. Chem. Soc.* **2000**, *122*, 3001–3006.
3. Hansen, U. M.; McClure, W. R. *J. Biol. Chem.* **1980**, *255*, 9564–9570.
4. Adams, R. L. P.; Knowler, J. T.; Leader, D. P. *The Biochemistry of the Nucleic Acids*; Chapman and Hall: London, 10th ed., Chapter 6.
5. Varmus, H. *Science* **1988**, *240*, 1427–1435.
6. Frisch, M. J. et al., *Gaussian 94 (revision E. 2)*; Gaussian, Inc.: Pittsburgh, PA, 1995.
7. (a) Sugiyama, H.; Saito, I. *J. Am. Chem. Soc.* **1996**, *118*, 7063–7068. (b) Saito, I.; Nakamura, T.; Nakatani, K.; Yoshioka, Y.; Yamaguchi, K.; Sugiyama, H. *J. Am. Chem. Soc.* **1998**, *120*, 12686–12687. (c) Yoshioka, Y.; Kitagawa, Y.; Takano, Y.; Yamaguchi, K.; Nakamura, T.; Saito, I. *J. Am. Chem. Soc.* **1999**, *121*, 8712–8719. (d) Prat, F.; Houk, K. N.; Foote, C. S. *J. Am. Chem. Soc.* **1998**, *120*, 845–846.
8. Fedoroff, O. Y.; Salazar, M.; Reid, B. R. *J. Mol. Biol.* **1993**, *233*, 509–523.
9. Conn, G. L.; Brown, T.; Leonard, G. A. *Nucleic Acids Res.* **1999**, *27*, 555–561.
10. (a) Gao, Y.-G.; Robinson, H.; van Boom, J. H.; Wang, A. H.-J. *Biophys. J.* **1995**, *69*, 559–568. (b) Robinson, H.; Wang, A. H.-J. *Nucleic Acids Res.* **1996**, *24*, 676–682. (c) Gao, Y.-G.; Robinson, H.; Wang, A. H.-J. *Eur. J. Biochem.* **1999**, *261*, 413–420.
11. Nunn, C. M.; Neidle, S. *J. Mol. Biol.* **1996**, *256*, 340–351.
12. Gyi, J. I.; Conn, G. L.; Lane, A. N.; Brown, T. *Biochemistry* **1996**, *35*, 12538–12548.